AMPLITUDO 5(1) (2026)
AMPLITUDO: Journal of Science & Technology Innovation
https://journals.balaipublikasi.id/index.php/amplitudo/index

Gamma Radiation Effects on SAC305 Lead-Free Solder for Space and Nuclear Electronics: XRD and Microstructural Evolution

Muhamad Mukhzani Muhamad Hanifah[1], Norliza Ismail[2], Azuraida Amat[3], Nurazlin Ahmad[3], Muhammad Nur Hisyam Rosman[3], Wilfred Paulus[4], Susilawati[5], Wan Yusmawati Wan Yusoff[3*]

[1]Faculty of Science and Defence Technology, Universiti Pertahanan Nasional Malaysia, Kem Sungai Besi, Kuala Lumpur, Malaysia
[2]UAS Research Cluster, Avionics Section, Malaysian Institute of Aviation Technology, Universiti Kuala Lumpur, Dengkil, Selangor, Malaysia.
[3]Department of Physics, Centre for Defence Foundation Studies, Universiti Pertahanan Nasional Malaysia, Kem Sungai Besi, Kuala Lumpur, Malaysia
[4]Malaysian Nuclear Agency, Bangi, Kajang, Selangor, Malaysia
[5]Physics Education Program, FKIP, University of Mataram, Mataram, Lombok Island, West Nusa Tenggara, Indonesia.

Received: December 11, 2025
Revised: February 04, 2026
Accepted: February 12, 2026
Published: February 28, 2026

Corresponding Author*:
Wan Yusmawati Wan Yusoff
yusmawati@upnm.edu.my

DOI: 10.56566/amplitudo.v5i1.531

Abstract: This study examines how gamma radiation (0–50,000 Gy) affects SAC305 (Sn-3.0Ag-0.5Cu) solder. Solder joints were irradiated using a Co-60 source. Structural changes were evaluated by X-ray diffraction and microstructural evolution were observed with optical microscopy after etching. XRD of *β*-Sn reflections indicates smaller crystallite size with dose, together with higher lattice strain and greater dislocation density, consistent with crystal-level alteration under irradiation. Microstructure observations show coarsening of *β*-Sn grains and thickening of the Cu_6Sn_5 intermetallic (IMC) layer at the Cu/solder interface as dose increases. These outcomes reveal a two-scale response: nanoscale coherent domains refine due to defect formation and accumulation, while microscale grains grow and the IMC layer thickens due to radiation-enhanced diffusion, which increases atomic mobility. Recognizing that the system involves different length scales helps resolve the apparent contradiction between the decreasing crystallite size and the increasing grain size. Practically, the combined increases in lattice strain, dislocation density, and IMC thickness may reduce reliability and fatigue life of SAC305 solder joints in high-radiation environments such as space and nuclear applications.

Keywords: β-Sn grain growth; Crystallite size; Dislocation density; Gamma radiation; Intermetallic layer; Lattice strain; Radiation-enhanced diffusion; Solder; X-ray diffraction.

Introduction

Solder joints are critical connections in electronic and electrical systems, serving as the bonds that connect components and enable the flow of electrical signals. These joints are formed by melting a solder alloy, traditionally tin–lead (SnPb) and, more recently, lead-free solders, to create a reliable and conductive connection between components such as wires, circuit boards, and electronic devices (Desmarest, 2012; Guan et al., 2023a). The importance of solder joints lies in their ability to provide both mechanical support and electrical continuity, ensuring a low-resistance current path while maintaining the physical stability of electronic assemblies (Choi et al., 2025; Guan et al., 2023b). High-quality solder joints reduce the risk of electrical failures such as open circuits, short circuits, and premature device breakdown, thereby improving the durability and service life of electronic products (Dele-Afolabi et al., 2023; Jiang et al., 2019; Li et al., 2024). Consequently, reliable solder joints are essential across a wide range of

How to Cite:
Hanifah, M. M. M., Ismail, N., Amat, A., Ahmad, N., Rosman, M. N. H., Paulus, W., … Yusoff, W. Y. W. (2026). Gamma Radiation Effects on SAC305 Lead-Free Solder for Space and Nuclear Electronics: XRD and Microstructural Evolution. *AMPLITUDO: Journal of Science and Technology Innovation*, *5*(1), 158-167. https://doi.org/10.56566/amplitudo.v5i1.531

applications, including consumer electronics, aerospace, automotive, and industrial systems (Maniar et al., 2020).

The widespread use of lead-free solders has increased due to environmental and health concerns associated with lead-containing materials. International regulations, such as the Restriction of Hazardous Substances (RoHS) directive, have significantly limited the use of SnPb solders and accelerated the transition toward lead-free alternatives(Muhamad Hanifah et al., 2025). Among these, tin–silver–copper (Sn–Ag–Cu) alloys, particularly Sn–3.0Ag–0.5Cu (SAC305), have become the most commonly used lead-free solder because of their acceptable melting temperature, good mechanical properties, and compatibility with existing manufacturing processes. As a result, SAC305 has become the dominant solder alloy in modern electronic assemblies, making it necessary to understand its long-term reliability under harsh operating conditions, including radiation exposure.

Research on the effects of gamma radiation on solder joints is of great importance due to its relevance to several critical industries. In aerospace applications, electronic components are exposed to high levels of ionizing radiation in space, and the reliability of solder joints is essential for mission success and system longevity. Similarly, in nuclear facilities, electronic control and monitoring systems depend on stable solder joints, where radiation-induced failure could lead to serious safety risks. In medical devices, particularly those used in radiation imaging and therapy, solder joint reliability directly affects patient safety and treatment accuracy. Military and defense systems are also exposed to radiation in extreme environments, requiring dependable solder joints to maintain operational performance (Coyle et al., 2015).

Among various types of ionizing radiation, gamma radiation is particularly significant due to its extremely high penetrating power, which allows it to affect materials throughout their entire volume. Gamma radiation induces material damage primarily through energy transfer mechanisms such as Compton scattering, leading to defect formation and structural degradation (Paulus et al., 2015; Yusoff et al., 2021). Furthermore, gamma radiation is one of the most common forms of ionizing radiation encountered in space and nuclear environments, making it highly relevant for evaluating the radiation tolerance of solder joints.

Previous studies have extensively examined the impact of gamma radiation on solder alloys and solder joints, revealing alterations in both microstructure and mechanical properties (Ismail et al., 2024; Lehan et al., 2022a; Lehan et al., 2022b; Wan Yusoff et al., 2023; Wang et al., 2018, 2019; Wen et al., 2020). Wang et al. (2018) found minimal effects of gamma ray irradiation on the intermetallic compound (IMC) layer's thickness and morphology in Sn63Pb37/Cu solder joints. However, the mechanical properties significantly degraded due to the formation of micro-voids and micro-cracks, leading to an 11.47% reduction in shear force and decreased ductility. These micro-voids and micro-cracks were consistently observed in irradiated solder joints, both in Sn-Pb and Pb-free solder alloys, as supported by multiple studies (Guan et al., 2023b; Wang et al., 2019). Wen et al. (2020) also noted that the size and quantity of voids increased with prolonged irradiation.

Studies focusing on lead-free SAC305 solder joints revealed comparable degradation trends. Lehan et al. (2022a) reported that increasing gamma radiation doses caused SAC305 joints to become softer and more ductile, with microstructural changes identified using field emission scanning electron microscopy (FESEM) and energy dispersive spectroscopy (EDS), including the presence of Cu_6Sn_5 and Ag_3Sn intermetallic compounds. These microstructural changes led to reduced hardness and elastic modulus. Yusoff et al. (2021) and Rosman et al. (2024) confirmed radiation-induced changes in hardness and creep behavior, where defect generation contributed to material hardening and altered creep rates across radiation doses ranging from 10 Gy to 50 Gy. Guan et al. (2023b) observed oxidation of β-Sn to SnO_2 under gamma irradiation, with micro-cracks forming at SnO_2/β-Sn interfaces.

Although these studies provide valuable insights into radiation-induced microstructural and mechanical changes, a clear understanding of the underlying crystallographic damage in SAC305 solder joints remains limited. In particular, systematic analysis of crystal-level parameters, such as crystallite size, lattice strain, and dislocation density, and their evolution under a wide range of gamma radiation doses has not been fully explored. Moreover, the relationship between crystallographic changes and observed microstructural degradation has not been clearly established.

X-ray diffraction (XRD) offers a non-destructive, straightforward, and budget-friendly method for determining the crystal structure of materials. This makes XRD particularly valuable for studying how gamma radiation affects solder alloys. For instance, research by Paulus et al. (2017) showed that XRD can detect changes in the crystallite size of β-Sn grains, which correlate with variations in the hardness of solder joints exposed to radiation.

This study utilizes XRD to examine SAC305 solder joints, specifically focusing on how a wide range doses of gamma radiation impacts their crystal structure and microstructure. The goal is to gain a comprehensive understanding of the structural transformations these solder joints undergo at different radiation levels, ultimately uncovering the mechanisms driving these changes.

Through meticulous characterization and in-depth analysis, this study will not only provide insights into the specific effects of radiation on SAC305 solder joints but also contribute to a broader understanding of how solder joints behave under extreme conditions. This knowledge will lay the foundation for future research and practical applications in this field.

Method

Sample preparation

In this study, SAC305 solder paste was used to form solder joints on Cu pads of a printed circuit board (PCB) via manual stencil printing. The printed solder underwent reflow soldering consisting of preheat, soak, reflow, and cooling (Figure 1).

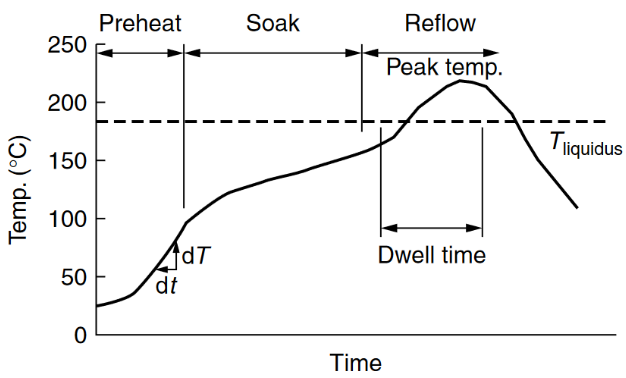

Figure 1 Reflow profile for soldering process

i. Preheat: temperature raised to ~100 °C at a controlled rate to avoid thermal shock and allow solvent evaporation.
ii. Soak: held at 100–150 °C for 60–120 s to ensure uniform heating and flux activation.
iii. Reflow: temperature increased to ~240 °C for 20–40 s to fully melt the solder and form joints.
iv. Cooling: rapid, controlled cooling to solidify joints while minimizing thermal stress.

After reflow process, cross sections of specimens for analysis were prepared using metallography technique. For diffraction and microscopy, measurements were restricted to the solder layer (β-Sn matrix and its second phases) in the central region of the joint, avoiding the Cu substrate and interface IMC to ensure that the XRD and optical microscope (OM) data represent the solder material.

Gamma radiation exposure

For gamma radiation exposure, the Gamma cell (Excel 220) gauge was used to radiate the samples by applied Cobalt-60 source. The samples were sealed inside the sample holder which was then inserted into the Gamma cell radiation chamber. The instantaneous source activity $A(t)$ was calculated from the initial activity A_0 using:

$$A(t) = A_0 e^{-\lambda t} = A_0 \left(\tfrac{1}{2}\right)^{-\frac{t}{T_{1/2}}} \quad (1)$$

where λ is the decay constant $\left(\frac{\ln 2}{T_{1/2}}\right)$ and $T_{1/2}$ is the half-life of Co-60.

The dose rate $D^{\cdot}$ was obtained from the facility calibration (proportional to $A(t)$ and geometry). The total absorbed dose D was computed as:

$$D = D^{\cdot} \times t_{exp} \quad (2)$$

where t_{exp} is the exposure time. Thus, exposure time for a target dose is:

$$t_{exp} = \frac{D}{D^{\cdot}} \quad (3)$$

The solder was exposed to gamma radiation at five different doses: 5, 50, 500, 5000 and 50000 Gy, with a specific dose rate of 0.8427 kGy/hr. Exposure time for each dose were tabulated in Table 1. After the exposure, the samples were carefully stored in a dry box to prevent any potential contamination or oxidation. The samples then proceeded with microstructural observation and XRD analysis.

Table 1. Exposure time for each gamma dose

Gamma dose (Gy)	Exposure time (s)
5	21.35
50	213.67
500	2136.75
5000	21367.52
50000	213675.20

Microstructural and phase analysis

Samples were subjected to metallography techniques for microstructure observation. This involved a sequence of steps including mounting, cross-sectioning, grinding, polishing, and etching. The samples were first cold mounted using epoxy and subsequently ground with silicon carbide (SiC) paper of grit sizes 400, 600, 800, and 1200. Following grinding, the samples underwent polishing using a polishing cloth and 1 µm and 0.25 µm diamond spray. Subsequently, the samples were etched using a solution of 5% hydrochloric acid and 95% methanol. Microstructural observations were performed with an Eclipse M200 optical microscope, focusing on the solder matrix (β-Sn grains). ImageJ was used to measure β-Sn grain size and IMC layer thickness at the Cu/solder interface (for joint cross-sections). The phase constituents of both the control sample and irradiated samples were analyzed using XRD equipment, specifically the X'Pert Pro MPD model from PANalytical, with a CuKα1 radiation source (λ= 1.5406 Å) and an angle 2θ in the range 20° to 80°. The collected data were then processed using X'Pert HighScore Plus to perform background subtraction, peak identification, and peak fitting. The most prominent peak corresponding to the JCPD was selected for analysis. Other than phase identification, XRD line-profile analysis was used to evaluate crystal-level parameters indicative of radiation damage: crystallite size, lattice strain, and dislocation density (e.g., Williamson–Hall or Warren–Averbach approaches applied to dominant β-Sn reflections). These parameters enable quantitative assessment of gamma-induced lattice disorder.

Result and Discussion

XRD analysis

XRD was used to study the effect of a wide range of gamma doses on the crystal structure of SAC305 solder joints. The XRD patterns of the as-soldered (0 Gy) and irradiated (5, 50, 500, 5000, 50000 Gy) samples are shown in Figure 2.

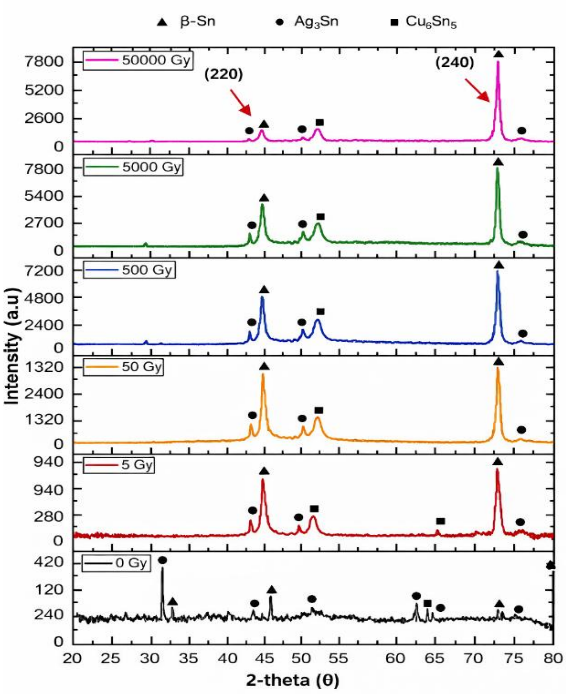

Figure 2. XRD spectra of SAC305 solder joints on selected gamma doses 0 Gy, 5 Gy, 50 Gy, 500 Gy, 5000 Gy and 50000 Gy

The detected peaks correspond to the β-Sn matrix with weaker reflections that are consistent with Ag_3Sn and Cu_6Sn_5 intermetallic phases reported in SAC305 by previous researchers. As the primary phase, β-Sn gives multiple distinct peaks in the pattern. In Figure 2, the presence of β-Sn is evident from clear reflections indexed as (220) and (240). For the as-soldered sample, β-Sn (220) and (240) appear at 2θ ≈ 45.24° and 72.67°, respectively. After irradiation, the β-Sn (220) peak shows a small shift to lower 2θ, while β-Sn (240) remains approximately at its original position. Because β-Sn is the dominant phase in SAC305, further analysis focused on intensity, crystallite size, dislocation density, and lattice strain for these peaks.

The intensity values, crystallite size, dislocation density and lattice strain of both β-Sn peaks was shown in Figure 3, 4, 5 and 6 respectively. The intensity values for β-Sn (220) and (240) are shown in Figure 3. Intensity in XRD is affected by several factors including phase fraction, preferred orientation (texture), surface flatness, effective irradiated volume, and micro absorption, in addition to crystal defects. In our study, we observed significant variations in intensity as the gamma radiation dose increased. Based on Figure 3, intensity of both β-Sn peaks suddenly starts to spike at dose 50 Gy. The increasing intensity with higher radiation doses suggests a transition towards a more ordered and crystalline structure (Mannan et al., 2006). However, increased peak intensity should not be interpreted as a "more ordered" crystal in this context. The line-profile results show higher micro strain and increased dislocation density with dose—both indicators of greater lattice disorder. Therefore, the intensity change is more reasonably attributed to texture evolution or surface/geometry effects introduced during preparation and irradiation, rather than to improved crystallinity (Ungár, 2004).

Gamma radiation induces changes in the crystal structure of β-Sn, which are reflected in the intensity peaks of the XRD pattern. Further analysis on XRD data was performed to determine the average crystallite size and dislocation density of primary phase β-Sn. Crystallite size, a measure of the dimensions of individual crystalline domains, is a critical parameter affecting the material's mechanical properties and performance. In this study, crystallite size was determined by using the following Debye-Scherer equation 3.

$$D_{ave} = K \times \frac{\lambda}{\beta} \times \cos(\theta) \quad (4)$$

where K represents the Scherrer constant (0.98), λ is XRD wavelength, β is the full width at half maximum (FWHM) and θ is the Bragg angle calculated as half of the peak position. The average crystallite size obtained for unirradiated and irradiated solder were indicated in

Figure 4. Based on Figure 4, average crystallite size exhibited variations with increasing gamma radiation doses. After expose to the gamma radiation at 5 Gy dose, crystallite size for β-Sn with 220 planes slightly increase before decrease at higher gamma dose after that. Meanwhile for β-Sn with 240 planes the trend of crystallite size decrease and slightly fluctuates just after gamma radiation was introduced to the solder alloy. Gamma radiation can reduce the crystallite size of β-Sn through radiation-induced recrystallization (Kassim et al., 2023).

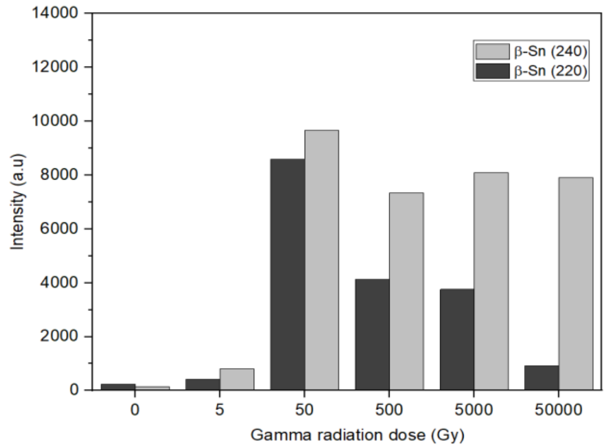

Figure 3. Intensity of both 220 and 240 β-Sn peaks under varied gamma radiation dose

Based on the average particle size values obtained from equation 4, the dislocation density value of investigated peaks can be determined. The dislocation density (δ) can be calculated using equation 5. δ value denotes the number of dislocation lines per unit volume of crystal, which is the size of the crystal defects possessed by a crystal. In other words, the dislocation density value will illustrate the degree of crystallinity of the material

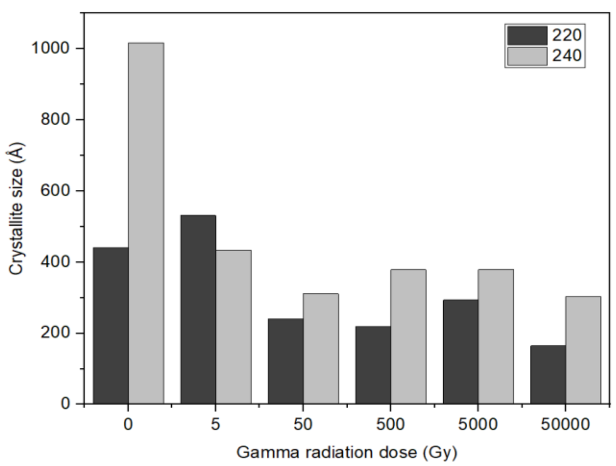

Figure 4. Crystallite size of both 220 and 240 β-Sn peaks under varied gamma radiation dose

$$\delta np = \frac{1}{D^2} \quad (5)$$

The dislocation density, a measure of the concentration of linear defects within the crystal lattice, is a key parameter that impacts the mechanical properties of the material (Prasad et al., 2021). Figure 5 show the dislocation density for both peaks. Our data demonstrated changes in dislocation density in response to gamma radiation exposure. The increased dislocation density indicates the presence of radiation-induced structural changes and defects. These defects can significantly influence the material's mechanical properties, including its strength and ductility (Rahman et al., 2020; Zheng et al., 2023). The unique responses of the 220 and 240 planes highlight the importance of understanding their distinct behaviors under radiation exposure. Further investigations are required to reveal the underlying mechanisms driving the observed variations and their implications for practical applications.

Lattice strain refers to the distortion or deformation within the crystal lattice of a material. In a crystalline material, atoms are arranged in a highly ordered, repeating pattern known as the crystal lattice. When this lattice is subject to external influence such as gamma radiation or the presence of defects, the regular arrangement of atoms can be disrupted, leading to lattice strain (Egami et al., 2015; Mote et al., 2012). Lattice strain (ε) is related to the Scherrer broadening in XRD analysis. The relationship between lattice strain and the Scherrer broadening can be expressed as follows:

$$\varepsilon = \frac{K\lambda}{\beta \bullet \cos(\theta)} \quad (6)$$

where ε represents the lattice strain. K is the Scherrer constant, typically between 0.9 and 1.0, accounting for factors related to the crystal structure. λ is the wavelength of the X-ray used for diffraction. β is the full width at half maximum (FWHM) of the diffraction peak. θ is the Bragg angle.

Figure 6 illustrates that the lattice strain of both β-Sn peaks increases following exposure to gamma radiation. The data shows noticeable changes in lattice strain as the gamma radiation dose increases. This implies that gamma radiation causes structural changes, resulting in distortions within the lattice of the material. These changes are often linked to the introduction of imperfections such as defects or dislocations, or even alterations in how atoms are arranged within the material (Debelle et al., 2018; Jossou et al., 2022). Additionally, the material's response varies between different crystal planes, as highlighted by the differing reactions of the 220 and 240 planes.

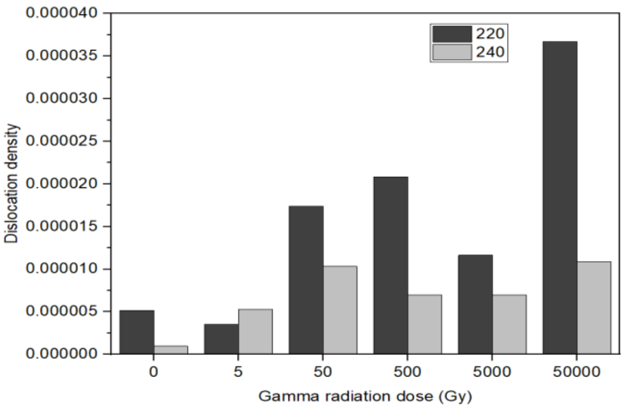

Figure 5. Dislocation density of both 220 and 240 β-Sn peaks under varied gamma radiation dose

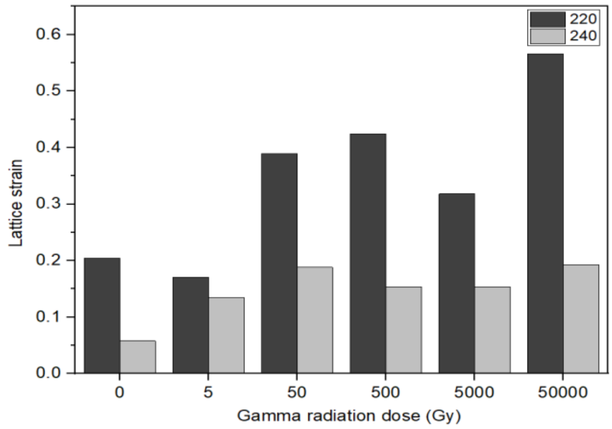

Figure 6. Lattice strain of both 220 and 240 β-Sn peaks under varied gamma radiation dose

The observed decrease in crystallite size, together with the increase in microstrain and dislocation density, can be explained by radiation-enhanced diffusion (RED) and defect-mediated processes under gamma irradiation, rather than by a macroscopic temperature increase. Gamma rays interact primarily through Compton scattering and pair production, generating point defects and defect clusters that increase atomic mobility at relatively low temperatures. This enhanced diffusivity promotes precipitate/IMC coarsening, interface reactions, and defect rearrangement, while breaking up the coherent domains into smaller regions at the nanoscale. This shows that RED explains the changes without needing any significant heating of the specimen.

Microstructure analysis

Figure 7 illustrates the optical micrographs of SAC305 solder joints under different variation of gamma dose. As can be seen, SAC305 solder matrix contains the primary β-Sn phase and is surrounded with the near eutectic phase (mixture of β-Sn and Ag_3Sn phase) and with the existence of Cu_6Sn_5 intermetallic compound layer (IMC) as established by previous literatures (Ismail et al., 2021). Ag_3Sn rod like precipitates usually embedded in the tin rich solid solution to form near eutectic phase. The unexpected strength of SAC material is due to the fine dispersion of rod-like Ag_3Sn particles in the Sn matrix (Silva et al., 2022). When exposed to a wide range of gamma doses, the evolution of the phases in the solder matrix especially β-Sn and near eutectic can be clearly observed.

Figure 8 illustrates the fluctuations in β-Sn grain size following exposure to gamma radiation. Exposure to gamma radiation induces the coarsening of β-Sn grains, which is evidenced by grain growth. Gamma radiation has the capability to promote grain growth in various materials. Consequently, this exposure results in the enlargement of individual grains or crystalline regions within the beta tin over time. This process is significant as it demonstrates the impact of gamma radiation on the microstructure of materials, leading to an increase in grain size and potentially affecting the material's properties and performance. The observation of grain growth in β-Sn due to gamma radiation is marked by a notable increase in grain size, indicating that gamma radiation can effectively drive the growth of crystalline regions in the material. This phenomenon highlights the transformative effect of gamma radiation on the material's internal structure, emphasizing the importance of understanding radiation-material interactions for various applications (Cunningham et al., 2021).

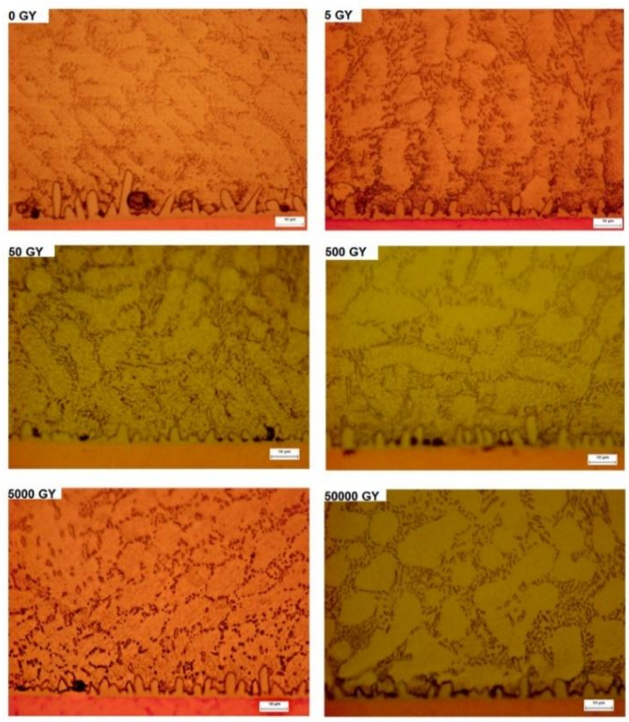

Figure 7. Micrograph of SAC305 solder under varied gamma doses a) 0 Gy b) 5 Gy c) 50 Gy d) 500 Gy e) 5000Gy f) 500000 Gy

Similarly, the IMC layer formed at the interface between the solder and the Cu substrate exhibits changes due to gamma radiation exposure. As depicted in Figure 8, the thickness of the IMC layer increases with higher doses of gamma radiation. Increased doses correlate with longer durations of radiation exposure. The increased effective diffusivity due to radiation-generated defects facilitates Cu transport from the substrate into the solder and Sn transport toward the interface, leading to faster Cu_6Sn_5 layer growth. Therefore, the dose-dependent IMC thickening is attributed to radiation-enhanced diffusion. Consequently, this enhanced diffusion promotes the growth of the IMC layer, resulting in its increased thickness. This process underscores the significant impact of gamma radiation on the microstructural evolution of the solder joint, with higher radiation doses leading to more pronounced changes in the IMC layer thickness (Ismail et al., 2024; Yusoff et al., 2021).

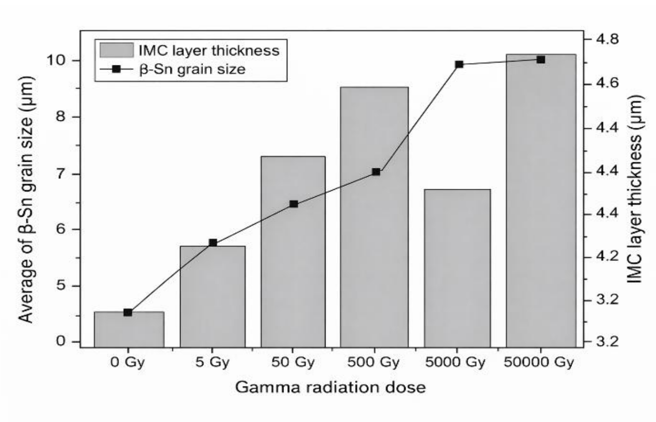

Figure. 8 Average of β-Sn grain size and IMC layer thickness of SAC305 solder under varied gamma radiation doses

Although XRD analysis reveals a decrease in crystallite size accompanied by increased microstrain and dislocation density with increasing gamma irradiation dose, optical microscopy observations of SAC305 solder may indicate apparent grain coarsening at the microscale. These findings are not contradictory, as they reflect microstructural evolution occurring across different length scales. The crystallite size obtained from XRD corresponds to coherently diffracting (coherently scattering) domains rather than the optical grain size, and is therefore highly sensitive to subgrain boundaries, dislocation structures, and low-angle misorientations that can exist within micron-scale grains (Leoni, 2019; Ungár, 2004). Under irradiation, the formation of irradiation-induced defects and defect arrangements (e.g., dislocation walls/subgrain structures) can reduce the coherent domain size even when the parent grains observed by optical microscopy appear coarser, because loss of coherence can occur without requiring a fully developed high-angle grain boundary (Ungár et al., 2005).

The observed microstructural changes are most consistently attributed to defect-mediated processes and radiation-enhanced diffusion rather than to any macroscopic temperature increase. In irradiated metals and alloys, ionizing radiation primarily generates excess point defects and defect clusters beyond thermal equilibrium, which can significantly enhance atomic mobility and diffusion when these defects are mobile, even under near-ambient or low-temperature conditions (Rivière, 1986). Recent studies have further demonstrated that irradiation can drive pronounced microstructural evolution through athermal defect dynamics, enabling stress relaxation and defect reorganization without reliance on thermally activated diffusion mechanisms (Feichtmayer et al., 2024). Accordingly, the irradiation-driven evolution observed in the present SAC305 solder system is interpreted as arising predominantly from defect generation and defect-assisted atomic transport rather than from thermally driven recovery or recrystallization.

Radiation-enhanced diffusion can also influence interfacial reactions between SAC305 solder and the Cu substrate. An increased defect density within the solder matrix and at/near the interface can provide fast diffusion pathways that promote Cu and Sn transport, thereby accelerating the growth kinetics and morphological evolution of Cu–Sn IMC, particularly Cu_6Sn_5 and Cu_3Sn (Ismail et al., 2024; Johnson & Orlov, 1986). In SAC305/Cu systems, growth of the Cu_6Sn_5 layer is commonly associated with grain-boundary diffusion control, while Cu_3Sn growth is more strongly linked to bulk diffusion, underscoring the importance of available diffusion paths and the defect/grain-boundary network in governing IMC development (Lee & Chen, 2022; Wu et al., 2023). Thus, while microscale grain coarsening may be observed in the bulk solder, irradiation-induced defect activity can simultaneously refine coherent domains detected by XRD and alter stress and diffusion conditions near the solder/IMC interface (Ismail et al., 2024; Ungár et al., 2005).

The refinement of coherent domain size together with the increase in lattice strain implied by XRD peak broadening is expected to contribute to localized stress heterogeneity, which can couple with diffusion-controlled IMC growth to produce non-uniform Cu_6Sn_5 morphology and facilitate subsequent Cu_3Sn development under prolonged irradiation exposure (Lee & Chen, 2022; Wu et al., 2023). Consequently, the coexistence of grain coarsening observed by optical microscopy, coherent-domain refinement and increased lattice strain detected by XRD, and modified IMC growth behavior is consistent with a multiscale, defect-mediated, radiation-enhanced diffusion-driven microstructural evolution governed in part by athermal irradiation effects in gamma-irradiated SAC305 solder joints (Feichtmayer et al., 2024; Ismail et al., 2024; Leoni, 2019; Ungár et al., 2005).

The material's reaction to gamma radiation reveals its high sensitivity and complex response. There are strong connections between increased radiation exposure and various changes within the material involving high intensity peaks in XRD, smaller crystallite size, higher dislocation density and strain in the structure, coarsening of the microstructure including IMC layer. These correlations suggest a complete transformation of the material, affecting both its small-scale structure and larger grain arrangement. Understanding these connections is crucial for making the material perform better in places with lots of radiation and for customizing its properties for different uses. Further research is essential to fully grasp these connections and develop materials that can resist radiation-induced changes while meeting specific application needs.

Conclusion

In summary, XRD analysis of SAC305 solder exposed to gamma radiation evidenced crystal-level alterations, shown by a decrease in crystallite size and a dose-dependent increase in lattice strain and dislocation density. Complementary microstructural observations indicated coarsening of β-Sn grains and growth of the Cu_6Sn_5 IMC layer with dose. These results reveal a duality of response in which nanoscale coherent domains refine while microscale grains coarsen, a behavior consistent with RED rather than simple heating. Practically, the combined increase in lattice strain, dislocation density, and IMC thickness is expected to reduce the mechanical reliability and fatigue life of SAC305 solder joints in high-radiation environments (e.g., space and nuclear applications). Further work should quantify these links to mechanical performance and validate the RED-driven trends across broader dose rates and temperatures.

Acknowledgments
The authors gratefully acknowledge research funding from FRGS/1/2023/STG05/UPNM/02/1. The authors fully acknowledge Ministry of Higher Education (MOHE) and Universiti Pertahanan Nasional Malaysia for the approved fund that makes this important research viable and effective. The authors also appreciated Lynas Sdn. Bhd. for research materials and collaboration work

Author Contributions
Conceptualization, W.Y.W.Y. and N.I.; methodology, M.M.M.H. and N.I.; software, M.M.M.H.; validation, A.A., N.A., and W.P.; formal analysis, M.M.M.H.; investigation, M.M.M.H., N.A., and M.N.H.R.; resources, W.P.; data curation, M.M.M.H. and M.N.H.R.; writing—original draft preparation, M.M.M.H.; writing—review and editing, N.I., A.A., S. and W.Y.W.Y.; visualization, M.M.M.H.; supervision, W.Y.W.Y.; project administration, W.Y.W.Y.; funding acquisition, W.Y.W.Y. All authors have read and agreed to the published version of the manuscript.

Funding
This research funded from Ministry of Higher Education (MOHE) and Universiti Pertahanan Nasional Malaysia (FRGS/1/2023/STG05/UPNM/02/1).

Conflicts of Interest
The authors declare no conflict of interest

References (6 more)

Choi, S., Lim, S., Hanifah, M. M. M., Matteini, P., Yusoff, W. Y. W., & Hwang, B. (2025). An Introductory Overview of Various Typical Lead-Free Solders for TSV Technology. *Inorganics*, *13*(3), 1–13. https://doi.org/10.3390/inorganics13030086

Coyle, R. J., Sweatman, K., & Arfaei, B. (2015). Thermal Fatigue Evaluation of Pb-Free Solder Joints: Results, Lessons Learned, and Future Trends. *JOM*, *67*(10). https://doi.org/10.1007/s11837-015-1595-1

Cunningham, W. S., Hattar, K., Zhu, Y., Edwards, D. J., & Trelewicz, J. R. (2021). Suppressing irradiation induced grain growth and defect accumulation in nanocrystalline tungsten through grain boundary doping. *Acta Materialia*, *206*. https://doi.org/10.1016/j.actamat.2021.116629

Debelle, A., Crocombette, J. P., Boulle, A., Chartier, A., Jourdan, T., Pellegrino, S., Bachiller-Perea, D., Carpentier, D., Channagiri, J., Nguyen, T. H., Garrido, F., & Thomé, L. (2018). Lattice strain in irradiated materials unveils a prevalent defect evolution mechanism. *Physical Review Materials*, *2*(1). https://doi.org/10.1103/PhysRevMaterials.2.013604

Dele-Afolabi, T. T., Ansari, M. N. M., Azmah Hanim, M. A., Oyekanmi, A. A., Ojo-Kupoluyi, O. J., & Atiqah, A. (2023). Recent advances in Sn-based lead-free solder interconnects for microelectronics packaging: Materials and technologies. In *Journal of Materials Research and Technology* (Vol. 25, pp. 4231–4263). Elsevier Editora Ltda. https://doi.org/10.1016/j.jmrt.2023.06.193

Desmarest, S. G. (2012). Reliability of Pb-free solders for harsh environment electronic assemblies. In *Materials Science and Technology* (Vol. 28, Number 3).

https://doi.org/10.1179/026708311X13135951528964

Egami, T., Ojha, M., Khorgolkhuu, O., Nicholson, D. M., & Stocks, G. M. (2015). Local Electronic Effects and Irradiation Resistance in High-Entropy Alloys. *JOM*, *67*(10). https://doi.org/10.1007/s11837-015-1579-1

Feichtmayer, A., Boleininger, M., Riesch, J., Mason, D. R., Reali, L., Höschen, T., Fuhr, M., Schwarz-Selinger, T., Neu, R., & Dudarev, S. L. (2024). Fast low-temperature irradiation creep driven by athermal defect dynamics. *Communications Materials*, *5*(1). https://doi.org/10.1038/s43246-024-00655-5

Guan, Q., Hang, C., Li, S., Yu, D., Ding, Y., Wang, X., & Tian, Y. (2023). Research Progress on the Solder Joint Reliability of Electronics Using in Deep Space Exploration. In *Chinese Journal of Mechanical Engineering (English Edition)* (Vol. 36, Number 1). Springer. https://doi.org/10.1186/s10033-023-00834-4

Guan, Q., Hang, C., Yao, G., Li, S., Yu, D., Ding, Y., & Tian, Y. (2023). Effect of gamma irradiation on microstructural evolution and mechanical properties of Sn3Ag0.5Cu solder joints. *Journal of Materials Research and Technology*, *24*, 6022–6033. https://doi.org/10.1016/j.jmrt.2023.04.148

Ismail, N., Jalar, A., Abu Bakar, M., Safee, N. S., Wan Yusoff, W. Y., & Ismail, A. (2021). Microstructural evolution and micromechanical properties of SAC305/CNT/CU solder joint under blast wave condition. *Soldering and Surface Mount Technology*, *33*(1). https://doi.org/10.1108/SSMT-11-2019-0035

Ismail, N., Wan Yusoff, W. Y., Abdul Manaf, N. A., Amat, A., Ahmad, N., & Salleh, E. M. (2024). A comprehensive review of radiation effects on solder alloys and solder joints. In *Defence Technology* (Vol. 39, pp. 86–102). KeAi Communications Co. https://doi.org/10.1016/j.dt.2024.02.007

Ismail, N., Yusoff, W. Y. W., Lehan, N. F. N. M., Abdul Manaf, N. A., Amat, A., Ahmad, N., & Paulus, W. (2024). Microstructural evolution of 96.5Sn-3.0Ag-0.5Cu (SAC305) solder joints induced by variation doses of gamma-irradiation. *Journal of Materials Science: Materials in Electronics*, *35*(1). https://doi.org/10.1007/s10854-023-11749-0

Jiang, N., Zhang, L., Liu, Z. Q., Sun, L., Long, W. M., He, P., Xiong, M. Y., & Zhao, M. (2019). Reliability issues of lead-free solder joints in electronic devices. In *Science and Technology of Advanced Materials* (Vol. 20, Number 1, pp. 876–901). Taylor and Francis Ltd. https://doi.org/10.1080/14686996.2019.1640072

Johnson, R. A., & Orlov, A. N. (1986). *Physics of Radiation Effects in Crystals*. https://api.semanticscholar.org/CorpusID:92875595

Jossou, E., Assefa, T. A., Suzana, A. F., Wu, L., Campbell, C., Harder, R., Cha, W., Kisslinger, K., Sun, C., Gan, J., Ecker, L., Robinson, I. K., & Gill, S. K. (2022). Three-dimensional strain imaging of irradiated chromium using multi-reflection Bragg coherent diffraction. *Npj Materials Degradation*, *6*(1). https://doi.org/10.1038/s41529-022-00311-8

Kassim, H., Aljaafreh, M. J., Prasad, S., AlSalhi, M. S., Asemi, N. N., & Manikandan, E. (2023). Investigating the effect of gamma irradiation on the structural, optical, and electrical properties of bismuth-modified strontium titanate ceramics. *Journal of Materials Science: Materials in Electronics*, *34*(7). https://doi.org/10.1007/s10854-023-10039-z

Lee, J. Y., & Chen, C. M. (2022). Effects of Initial Morphology on Growth Kinetics of Cu6Sn5 at SAC305/Cu Interface during Isothermal Aging. *Materials*, *15*(14). https://doi.org/10.3390/ma15144751

Lehan, N. F. N. M., Yusoff, W. Y. W., Ahmad, K. Z. K., Ismail, N., Amat, A., Manaf, N. A. A., Abdullah, M. F., Jalar, A., Rahman, I. A., & Salleh, E. M. (2022). Influence of Gamma Radiation on Eutectic Phase Area and Hardness Properties of SAC305 Solder. *Jurnal Teknologi*, *84*(6–2), 113–118. https://doi.org/10.11113/jurnalteknologi.v84.19358

Lehan, N. F. N. M., Yusoff, W. Y. W., Sobri, N. S., Ahmad, K. Z. K., Abdullah, M. F., Amat, A., Jalar, A., Rahman, I. A., & Salleh, E. M. (2022). EDS analysis on effect of low dosage gamma radiation and micromechanical properties of SnAg3Cu0.5 solder. *Journal of Materials Science: Materials in Electronics*, *33*(7), 4225–4236. https://doi.org/10.1007/s10854-021-07617-4

Leoni, M. (2019). 5.1. Domain size and domain-size distributions. *International Tables for Crystallography*, *H*, 524–537. https://doi.org/https://doi.org/10.1107/97809553602060000966

Li, L., Du, X., Chen, J., & Wu, Y. (2024). Thermal Fatigue Failure of Micro-Solder Joints in Electronic Packaging Devices: A Review. In *Materials* (Vol. 17, Number 10). Multidisciplinary Digital Publishing Institute (MDPI). https://doi.org/10.3390/ma17102365

Maniar, Y., Konstantin, G., Sharma, A., Binkele, P., & Schmauder, S. (2020). Solder Joint Lifetime Modeling Under Random Vibrational Load

Collectives. *JOM*, *72*(2). https://doi.org/10.1007/s11837-019-03947-1

Mannan, A., Kazmi, K. R., Khan, M. S., & Khan, I. H. (2006). A method for the determination of relative crystallinity of minerals by X-ray diffraction. *Pakistan Journal of Scientific and Industrial Research*, *49*(2).

Mote, V., Purushotham, Y., & Dole, B. (2012). Williamson-Hall analysis in estimation of lattice strain in nanometer-sized ZnO particles. *Journal of Theoretical and Applied Physics*, *6*(1). https://doi.org/10.1186/2251-7235-6-6

Muhamad Hanifah, M. M., Ahmad Yusof, A. H., Amat, A., Ahmad, N., Yahya, A., Abdul Manaf, N. A., & Wan Yusoff, W. Y. (2025). Effect of La_2O_3 Doping on the Hardness, Microstructure and Void Formation of Sn-Ag-Cu (SAC305) Lead-Free Solder Alloys. *Solid State Science and Technology*, *33*(2), 119–126.

Paulus, W., Abdul Rahman, I., Jalar, A., Kamil Othman, N., Ismail, R., Wan Yusoff, W. Y., & Abu Bakar, M. (2017). The relationship between XRD peak intensity and mechanical properties of irradiated Lead-Free solder. *Materials Science Forum*, *888 MSF*, 423–427. https://doi.org/10.4028/www.scientific.net/MSF.888.423

Paulus, W., Rahman, I. A., Jalar, A., Kamil, I., Yusoff, W. Y. W., & Bakar, M. A. (2015). Effect of gamma radiation on micromechanical hardness of lead-free solder joint. *AIP Conference Proceedings*, *1678*. https://doi.org/10.1063/1.4931275

Prasad, K., Obana, M., Ito, A., & Torizuka, S. (2021). Synchrotron diffraction characterization of dislocation density in additively manufactured IN 718 superalloy. *Materials Characterization*, *179*. https://doi.org/10.1016/j.matchar.2021.111379

Rahman, M. M., Chen, W. Y., Mu, L., Xu, Z., Xiao, Z., Li, M., Bai, X. M., & Lin, F. (2020). Defect and structural evolution under high-energy ion irradiation informs battery materials design for extreme environments. *Nature Communications*, *11*(1). https://doi.org/10.1038/s41467-020-18345-4

Rosman, M. N. H., Yusoff, W. Y. W., Manaf, N. A. A., Abdullah, M. F., Abdullah, C. A. C., & Zyoud, S. H. (2024). An Investigation of the Effect of Wide Range Gamma Radiation from Nanoindentation of the SAC305 Solder Alloy. *Journal of Advanced Research in Micro and Nano Engineering*, *17*(1), 18–27. https://doi.org/10.37934/armne.17.1.1827

Silva, B. L., Mendes, P. H., Garcia, A., & Spinelli, J. E. (2022). Effect of Aging on Dendritic Array, Ag3Sn Spacing, and Hardness of a Sn-2Ag-0.7Cu Solder Alloy. *Journal of Electronic Materials*, *51*(8). https://doi.org/10.1007/s11664-022-09713-5

Ungár, T. (2004). Microstructural parameters from X-ray diffraction peak broadening. *Scripta Materialia*, *51*(8 SPEC. ISS.), 777–781. https://doi.org/10.1016/j.scriptamat.2004.05.007

Ungár, T., Tichy, G., Gubicza, J., & Hellmig, R. J. (2005). Correlation between subgrains and coherently scattering domains. *Powder Diffraction*, *20*(4), 366–375. https://doi.org/10.1154/1.2135313

Wan Yusoff, W. Y., Ismail, N., Mohmad Lehan, N. F. N., Amat, A., Ku Ahmad, K. Z., Jalar, A., & Abdul Rahman, I. (2023). Micromechanical response of SAC305 solder alloy under gamma radiation via nanoindentation approach. *Soldering and Surface Mount Technology*, *35*(1), 51–58. https://doi.org/10.1108/SSMT-09-2021-0060

Wang, J., Xue, S., Lv, Z., Wang, L., Liu, H., & Wen, L. (2018). Effect of gamma-ray irradiation on microstructure and mechanical property of Sn63Pb37 solder joints. *Journal of Materials Science: Materials in Electronics*, *29*(24), 20726–20733. https://doi.org/10.1007/s10854-018-0213-8

Wang, J., Xue, S., Lv, Z., Wen, L., & Liu, S. (2019). Microstructure and performance evolution of SnPbSb solder joint under γ-ray irradiation and thermal cycling. *Journal of Materials Science: Materials in Electronics*, *30*(5), 4990–4999. https://doi.org/10.1007/s10854-019-00795-2

Wen, L., Xue, S., Wang, L., Liu, H., & Wu, J. (2020). Microstructural evolution and shear performance of AuSn20 solder joint under gamma-ray irradiation and thermal cycling. *Journal of Materials Science: Materials in Electronics*, *31*(9), 7200–7210. https://doi.org/10.1007/s10854-020-03292-z

Wu, M., Wang, S. Lin, Yin, L. meng, Chen, Y. hua, Hong, M., Sun, W. Jun, Yao, Z. Xiang, Ni, J. Ming, Lu, P., Zhang, T. Ming, & Xie, J. Lin. (2023). Oxidation behavior and intermetallic compound growth dynamics of SAC305/Cu solder joints under rapid thermal shock. *Transactions of Nonferrous Metals Society of China (English Edition)*, *33*(10), 3054–3066. https://doi.org/10.1016/S1003-6326(23)66317-4

Yusoff, W. Y. W., Lehan, N. F. N. M., Sobri, N. S., Ahmad, K. Z. K., Jalar, A., & Rahman, I. A. (2021). Influences of low dose gamma radiation on hardness and microstructure properties of green solder joint. *Journal of Physics: Conference Series*, *1816*(1). https://doi.org/10.1088/1742-6596/1816/1/012118

Zheng, R., Xuan, W., Xie, J., Chen, S., Yang, L., & Zhang, L. (2023). The Evolution of Structural Defects under Irradiation in W by Molecular Dynamics Simulation. *Materials*, *16*(12). https://doi.org/10.3390/ma16124414